Electronic Supplementary Material (ESI) for ChemComm.

Electronic Supplementary Information (ESI)

Synthesis of amino-functionalized $Ti_3C_2T_x$ MXene by alkalization-grafting modification for efficient lead adsorption

Guoliang Zhang,*, [a] Tiecheng Wang,[a] Zehai Xu,[a] Minmin Liu,
[a] Chong Shen,[b] Qin Meng *, [b]

[a] *Institute of Oceanic and Environmental Chemical Engineering, State Key Lab Breeding Base of Green Chemical Synthesis Technology, Zhejiang University of Technology, Chaowang Road 18#, Hangzhou, Zhejiang 310014, China*

Tel/Fax: 86-571-88320863

[b]*College of Chemical and Biological Engineering, State Key Laboratory of Chemical Engineering, Zhejiang University, 38 Zheda Road, Hangzhou, Zhejiang 310027, China*

Tel/Fax: 86-571-87953193

**Corresponding author E-mail: guoliangz@zjut.edu.cn*

**Co-Corresponding author E-mail: mengq@zju.edu.cn*

Contents

1. Experimental detail
    1.1 Materials
    1.2 Methods
    1.3 Characterization
    1.4 Adsorption experiments
    1.5 Adsorption kinetics and isotherms
2. Results and Discussions
3. Reference

1. Experimental details

1.1 Materials

Ti_3AlC_2 powders were obtained from Beijing Materials Co., China. LiF, HCl, NaOH, ethyl alcohol, 3-aminopropyl triethoxysilane (APTES), lead acetate, liquid nitrogen and argon gas were purchased from the market. The deionized water was made by using the reverse osmosis device and the EDI unit.

1.2 Methods

Preparation of $Ti_3C_2T_x$, DL-MXene and alk-MXene. $Ti_3C_2T_x$ MXene was prepared by wet etching method.[1,2] In typical synthesis, LiF powders were immersed in HCl (9M) solutions to be dissolved, then the Ti_3AlC_2 powders were added slowly into the solution. Under argon gas atmosphere, the mixture was continuously stirred at 35℃ for 24 h. When Ti_3AlC_2 powers were fully etched, the solution was washed by deionized water and ethyl alcohol to remove HF and then centrifuged several times at 3500 rpm until the value of pH reach about 6.0. Subsequently, the obtained underlying precipitates were dried under vacuum at 80℃ overnight. Finally, the multilayer $Ti_3C_2T_x$ MXene was obtained. Delaminated MXene was obtained by ultrasonically exfoliating multilayer $Ti_3C_2T_x$ MXene in deionized water. The dispersion liquid was centrifuged at 3500 rpm for 45 min to separate the unexfoliated MXene. Finally, the supernatant was centrifuged at 8000 rpm for 30 min once again, and the bottom layer precipitate was vacuum dried to obtain delaminated MXene (labelled as DL-MXene). In the alkalization process, the prepared suspension liquid of DL-MXene were dispersed in a NaOH (5 wt%) solution and stirred at 20℃ for 4 h. After the alkalization reaction was completed, the mixture was washed 4-5 times to remove residual

NaOH. Finally, the wet sediment was vacuum dried at 80℃ for 8-10 h to obtain alkalized MXene samples, which were labelled as alk-MXene.

Preparation of alk-MXene-NH_2. The 0.1 g of alk-MXene powders were immersed in ethanol solution, and ultrasonically dispersed at room temperature. After the solution was completely dispersed, the APTES solution was instilled into the dispersed solution and then reacted for 6 h under argon. Afterwards, the mixture was centrifuged 5-6 times with the ethanol solution to completely remove excess APTES, and the precipitate at the bottom of the centrifuge tube was separated to dry overnight to obtain alk-MXene-NH_2 samples.

1.3 Characterization

The surface morphology of prepared samples was investigated by scanning electron microscope (SEM) analysis (SU8010, Hitachi) and transmission electron microscope (TEM) analysis (JEM-2100, JEOL, Japan). X-ray diffractometer (PNAlytical, Netherlands) was applied to perform X-ray powder diffraction (XRD) patterns at the scan step of 0.015° in the scan region of 5°-55° for 2θ. The BET surface area was analyzed by Brunauer-Emmet-Teller (Quantachrome, Autosorb-Iq-MP) date. The elemental analysis of different samples was studied by an energy dispersive spectroscope (EDS). The chemical composition of adsorbent samples was observed by Fourier-transform infrared spectrometer (FT-IR) via a Nicolet 6700 spectrometer (Thermo Nicolet, America) under the wavenumber range of 450 to 4000 cm^{-1}. A RBD upgraded PHI-5000C ESCA system (PerkinElmer) was applied to investigate X-ray photoelectron spectroscopy (XPS). The zeta potentials of MXene samples were performed by photon correlation spectroscopy via a Malvern Zetasizer 3000 HAS device.

1.4 Adsorption experiments

All adsorption experiments were performed in a 250mL beaker at room temperature under mild magnetic stirring. In a single experiment, 0.01g absorbent was added into 100mL Pb(II) solution (25mg L^{-1}), then sampled at different reaction times and filtered through a 0.45μm microporous membrane. The concentration of samples was measured by the atomic absorption spectroscopy (Varian spectra VARIAN55B). To explore the influence of pH values, the pH of reaction solution was adjusted from 1.0 to 6.3 by HCl and NaOH. Other heavy metal ions (Cu(II), Zn(II) and Ni(II)) adsorption experiments were performed with an initial metal concentration of 25 mg/L at 298K for 30 min. The competitive adsorption experiments were conducted similar to Pb(II) adsorption except that Pb(II) solution was replaced by Pb(II)/ Mg(II) or Pd(II)/ Ca(II) solution, in which the rations of lead ions to magnesium ions or calcium ions were 1:8, 1:16, 1:32, 1:64 and 1:128 while the concentration of lead ions was kept constant. The uptake capacity of various samples for Pb(II) was calculated by the following formula (Eq. 1):

$$Q=\frac{(C_0 - C_1)V}{m} \tag{1}$$

where Q represents the uptake capacity of lead ions (mg g^{-1}), C_0 is the initial concentration and C_1 is the residual concentration (mg L^{-1}) of lead ions in aqueous solution. m is the mass (g) of the absorbents and V is the volume (L) of aqueous solution.

The remove rate of Pb(II) was calculated by the following formula (Eq. 2):

$$R(\%)=\frac{C_0-C_1}{C_0}\times 100\% \tag{2}$$

where R is Pb(II) removal rate, C_0 is the initial concentration and C_1 is the residual concentrations (mg L^{-1}) of lead ions in aqueous solution.

1.5 Adsorption kinetics and isotherms

To investigate the adsorption behaviour of lead ions by alk-MXene-NH_2 over time under the constant condition, two equations of pseudo-first-order (Eq. 3) and pseudo-second-order (Eq. 4) were employed, which were showed respectively as follows:

$$\ln(q_e - q_t) = \ln q_e - \frac{k_1}{2.303} \tag{3}$$

$$\frac{t}{q_t} = \frac{1}{k_2 q_e^{\,2}} + \frac{t}{q_e} \tag{4}$$

where q_t represents the uptake capacity (mg g^{-1}) of adsorbent at time t and q_e represents uptake capacity (mg g^{-1}) of adsorbent at equilibrium; k_1 (min $^{-1}$) and k_2 (g mg^{-1} min^{-1}) are the rate constant of pseudo-first-order mode and pseudo-second-order mode, respectively; t is the adsorption time (min).

Meanwhile, to understand adsorption isotherms, the Langmuir (Eq. 5) and Freundlich isotherm (Eq. 6) modes were shown as follows:

$$\frac{1}{q_e} = \frac{1}{q_m K_L} \cdot \frac{1}{C_e} + \frac{t}{q_m} \tag{5}$$

$$\lg q_e = \lg K_F + \frac{1}{n} \cdot \lg C_e \tag{6}$$

where q_e represents the uptake capacity (mg g^{-1}) of adsorbent for heavy metal ions at equilibrium; q_m represents the maximum capacity (mg g^{-1}); C_e represents equilibrium concentration of lead ions; K_L (L mg^{-1}) and K_F (mg g^{-1}) are two constants of Langmuir and Freundlich, respectively; n is a heterogeneity factor which can reflect the influence of the adsorbent concentration to the adsorption capacity.

2. Results and Discussions

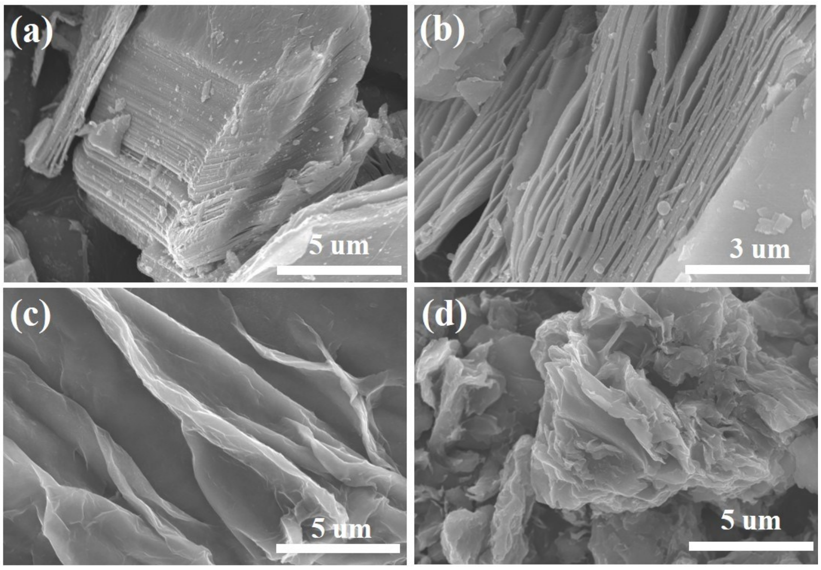

Fig. S1 SEM images of Ti_3AlC_2 (a), ML-MXene (b), DL-MXene (c) alk-MXene (d).

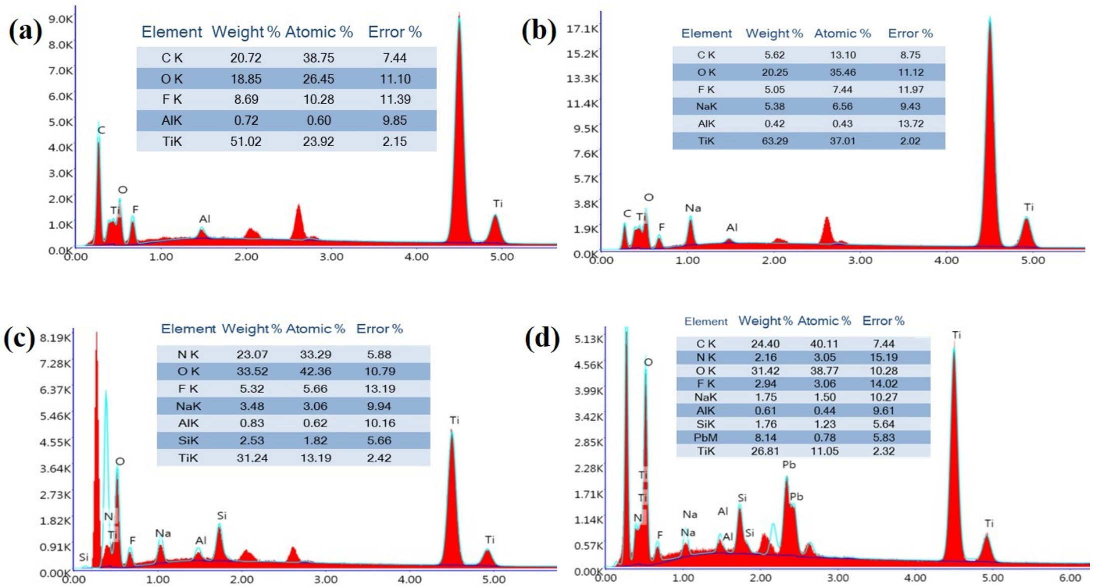

(a)

Element	Weight %	Atomic %	Error %
C K	20.72	38.75	7.44
O K	18.85	26.45	11.10
F K	8.69	10.28	11.39
AlK	0.72	0.60	9.85
TiK	51.02	23.92	2.15

(b)

Element	Weight %	Atomic %	Error %
C K	5.62	13.10	8.75
O K	20.25	35.46	11.12
F K	5.05	7.44	11.97
NaK	5.38	6.56	9.43
AlK	0.42	0.43	13.72
TiK	63.29	37.01	2.02

(c)

Element	Weight %	Atomic %	Error %
N K	23.07	33.29	5.88
O K	33.52	42.36	10.79
F K	5.32	5.66	13.19
NaK	3.48	3.06	9.94
AlK	0.83	0.62	10.16
SiK	2.53	1.82	5.66
TiK	31.24	13.19	2.42

(d)

Element	Weight %	Atomic %	Error %
C K	24.40	40.11	7.44
N K	2.16	3.05	15.19
O K	31.42	38.77	10.28
F K	2.94	3.06	14.02
NaK	1.75	1.50	10.27
AlK	0.61	0.44	9.61
SiK	1.76	1.23	5.64
PbM	8.14	0.78	5.83
TiK	26.81	11.05	2.32

Fig. S2 Elemental compositions of DL-MXene (a), alk-MXene (b), alk-MXene-NH_2 (c) and alk-MXene-NH_2 after Pb(II) adsorption (d).

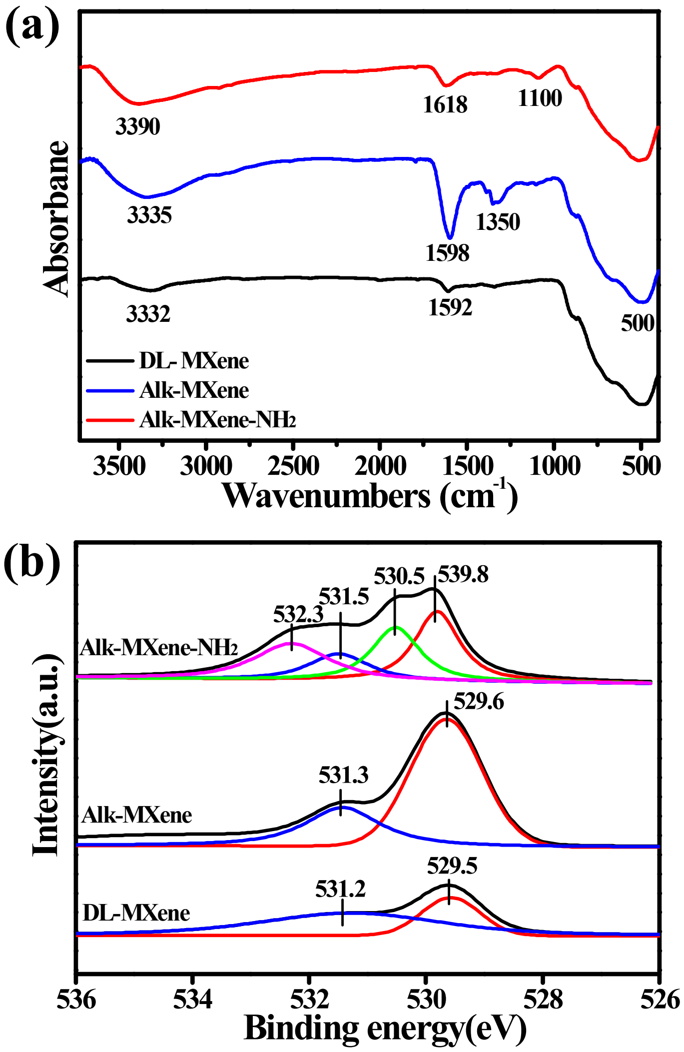

Fig. S3 FTIR spectra of MXene samples before and after amination modification (a). The O 1s spectra of prepared samples (b).

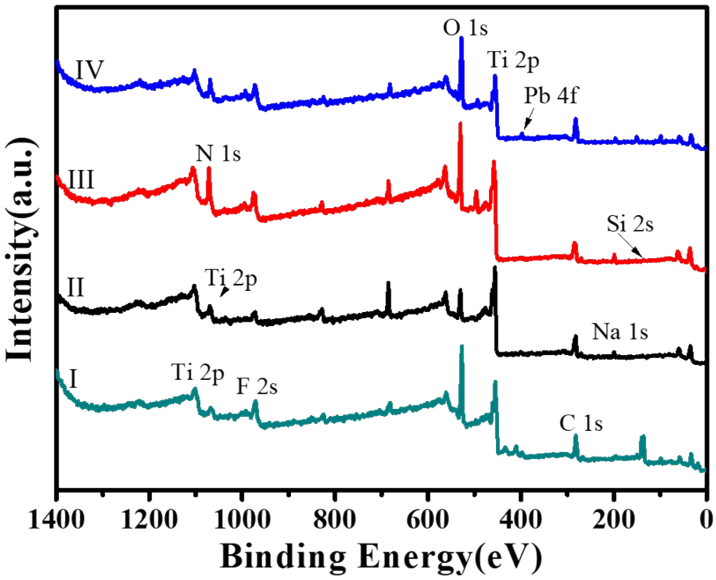

Fig. S4 XPS spectra of all MXene samples before and after adsorption of Pb(II): DL-MXene (I), alk-MXene (II), alk-MXene-NH_2 (III) and alk-MXene-NH_2 after Pb ions adsorption (IV).

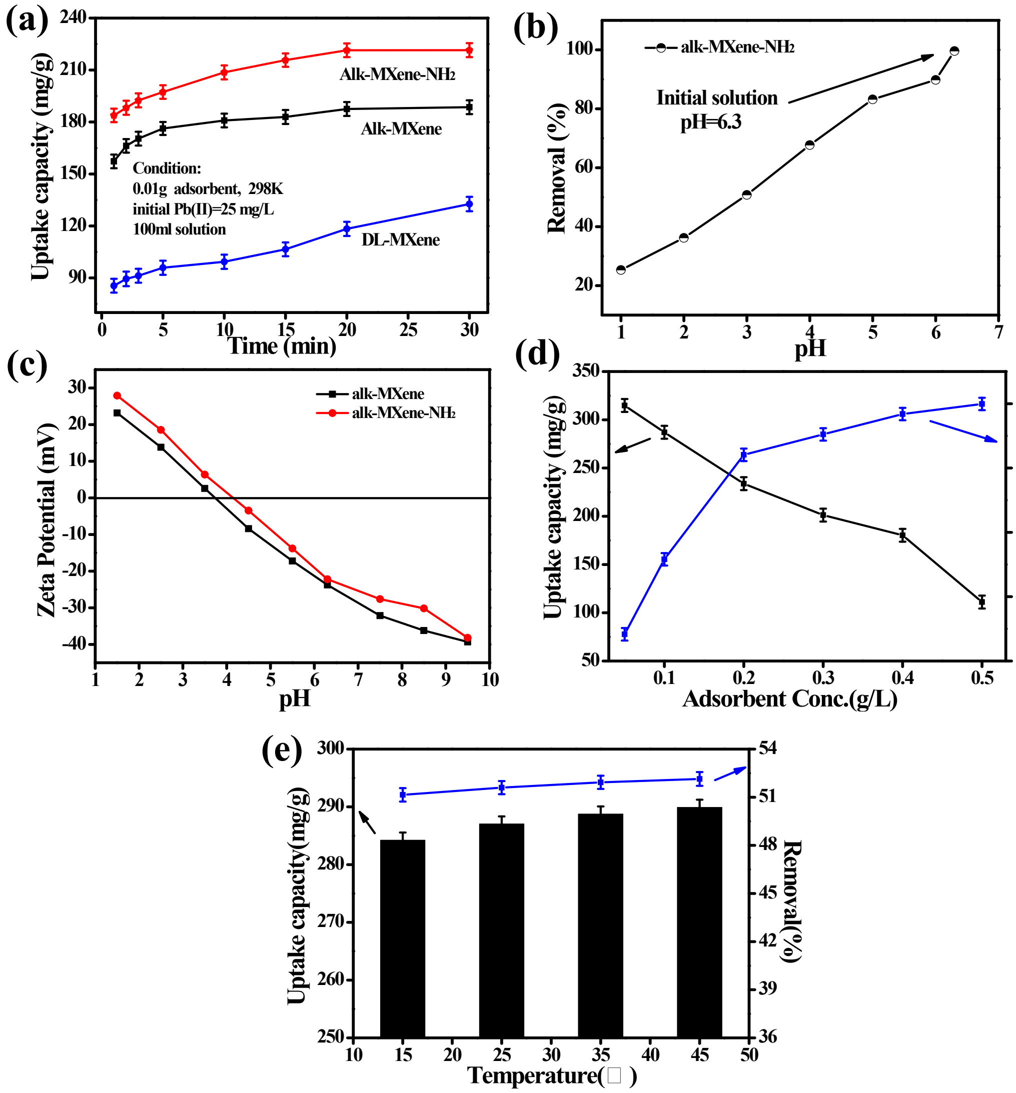

Fig. S5 Adsorption performance of different samples (a). Effect of pH on adsorption behaviors (b). Zeta potential of alk-MXene-NH$_2$ and alk-MXene samples (c), Effect of temperature and adsorbent concentration on adsorption behaviors (d,e).

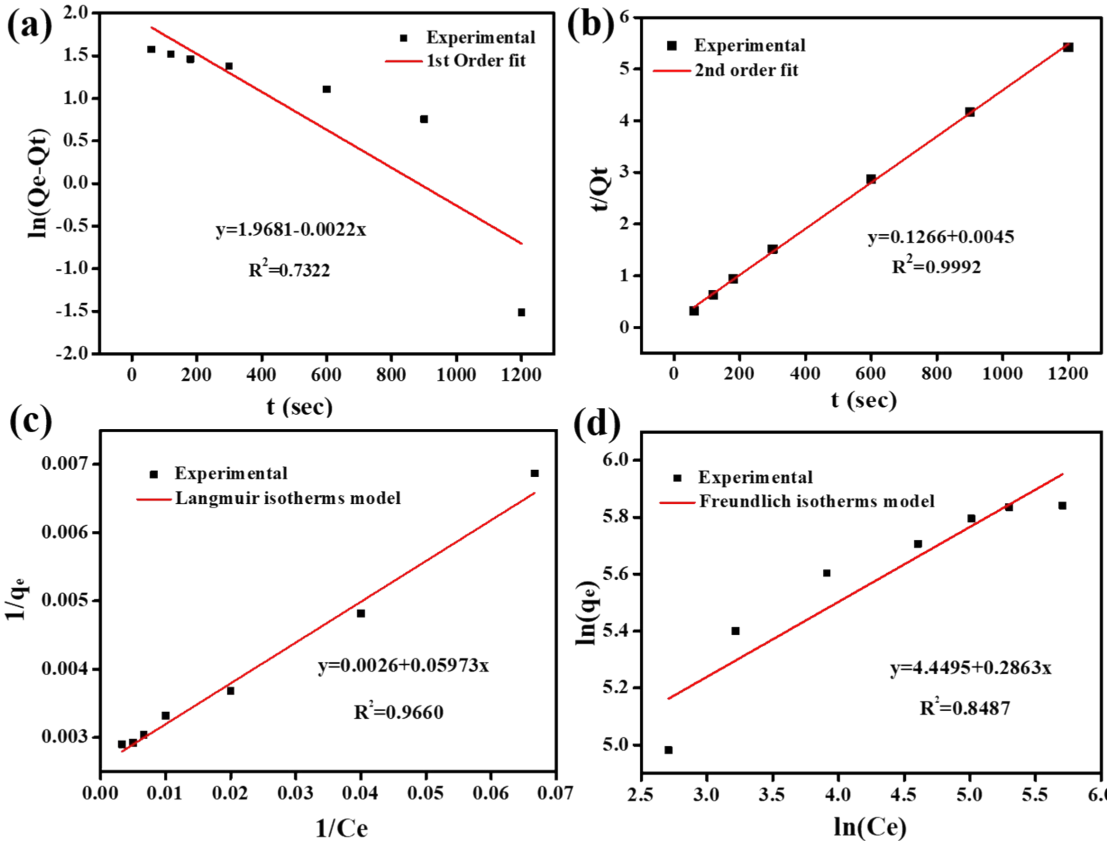

Fig. S6 Adsorption kinetic and isotherm models for Pb(II) adsorption at initial concentration of 25 mg L^{-1}: Pseudo-first-order kinetic line (a); Pseudo-second-order kinetic line (b); Langmuir isotherms model (c) and Freundlich isotherms model (d).

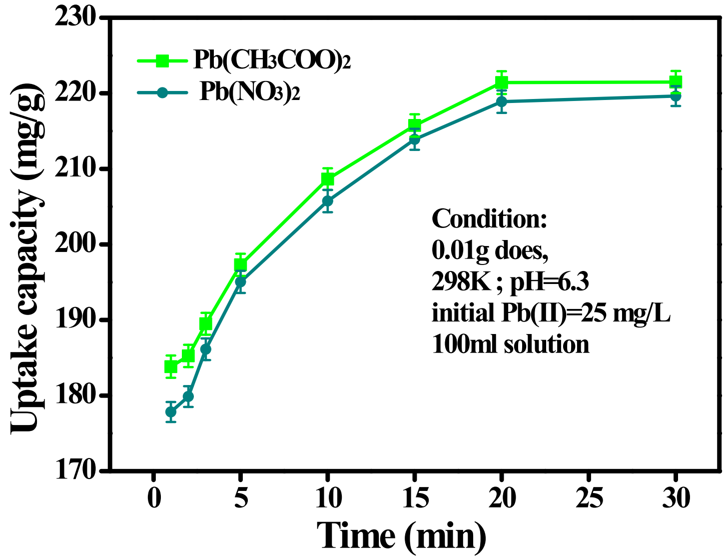

Fig. S7 The comparison of Pb(II) adsorption capacity in lead acetate and lead nitrate solutions.

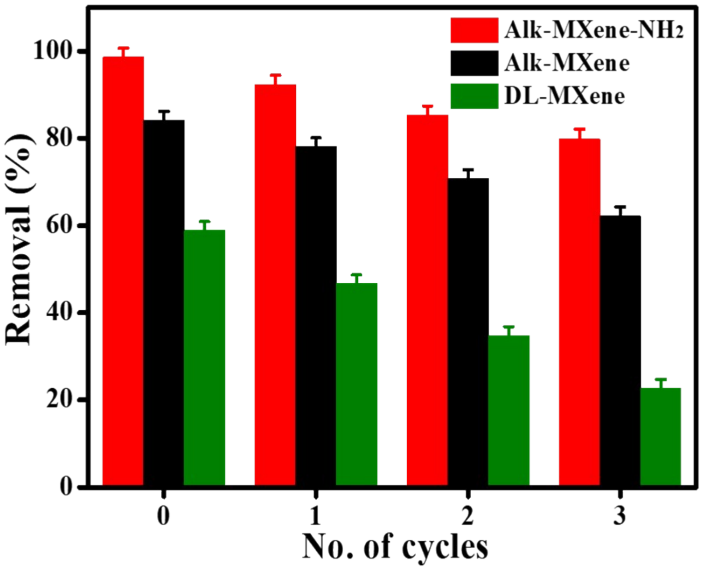

Fig. S8 Pb(II) adsorption capability by regenerated DL-MXene, alk-MXene and alk-MXene-NH_2 for three cycles (0.1 g L^{-1} adsorbent initial Pb(II) = 25 mg L^{-1}, pH = 6.1-6.4).

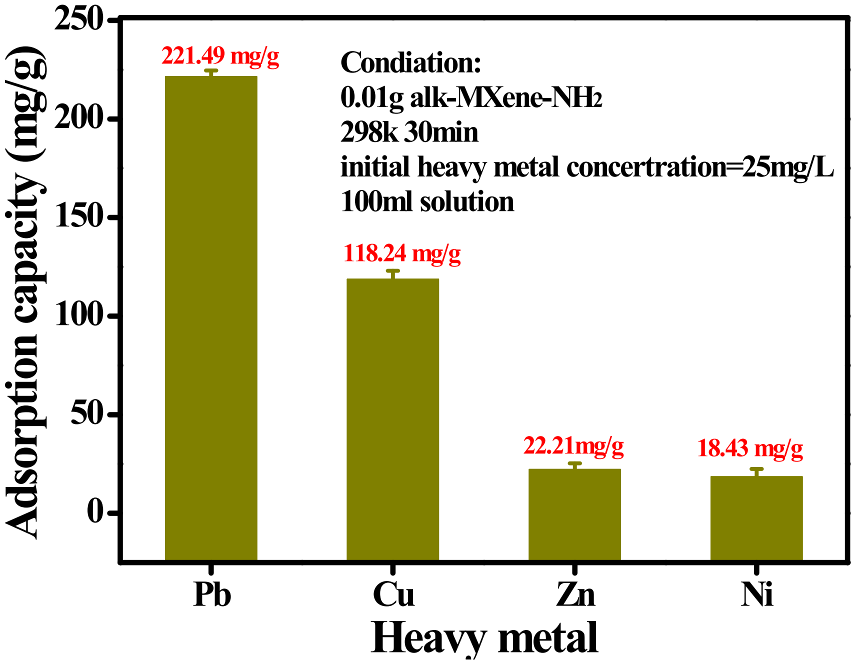

Fig. S9 The comparison of adsorption capacities for Cu(II), Zn(II) and Ni(II) by alk-MXene-NH_2.

Table. S1 Surface area and textural data of ML-MXene, alk-MXene and alk-MXene-NH_2 samples.

Sample	S_{BET} (m^2g^{-1})[a]	V_{meso} (cm^3g^{-1})[b]	Average pore diameter (nm)[c]
ML-MXene	6.37	0.0007	1.925
Alk-MXene	72.04	0.248	1.930
Alk-MXene-NH_2	129.21	0.517	1.912

[a] S_{BET} is the BET specific surface area.

[b] V_{meso} is the specific mesopore volume obtained from the BJH cumulative specific adsorption volume of pores of 1.54 to 38.61 nm in diameter.

[c] Average pore diameter is determined from the average of the BJH adsorption of pore diameters obtained in the adsorption branch of the N_2 isotherm.

Table. S2 Relative content of each element in different alk-MXene-NH_2 samples.

The concentration of APTES (mg/L)	Relative element content in alk-MXene-NH_2 samples (%)			
	Ti	C	N	Si
0.1	26.27	56.76	8.71	8.26
0.2	24.88	56.44	9.81	8.87
0.3	28.33	56.03	8.80	6.85

Table.S3 Kinetics model parameters and correlation coefficients for Pb (II) sorption on alk-MXene-NH_2.

Kinetics model	Kinetics model parameters		
	q_e (mg/g)	k	R^2
Pseudo-first-order model	92.918	k_1=0.0051 min^{-1}	0.7322
Pseudo-second-order model	222.222	k_2=0.00016g · $mg^{-1}min^{-1}$	0.9992
Equilibrium capacity from experiment	221.488 mg/g		

Table.S4 Adsorption isotherm parameters for Pb (II) adsorption onto alk-MXene-NH_2 at 298 K.

Adsorption isotherm	Parameter	value	R^2
Langmuir mode	K_L	0.044 L/mg	0.9660
	q_m	384.62mg/g	
Freundlich mode	n	3.49	0.8487
	K_F	85.57 L/mg	

Table S5 Comparison of Pb (II) ions adsorption capacities of different adsorbents.

Sample	Sorption Capacity (Q_{max} mg/g)	Equilibrium time/min	Ref.
$Ti_3C_2T_x$-KH570	147.29	30	3
Layered 2D alk-MXene	140	2	4
$Ti_3C_2T_x$ MXene	~35	30	5
EHL-$Ti_3C_2T_X$	239	300	6
1T-MoS_2	150	20	7
g-C_3N_4/MnO_2	104	250	8
Zn(Bim)(OAc)	253	180	9
T-NTO	328.9	240	10
O-TMU-40	215	120	11
Sulfur-doped -C_3N_4	52.63	120	12
Fe_3O_4/poly($C_3N_3S_3$)	232.6	20	13
Alk-MXene-NH_2	384.63	20	this work

3. References

1 M. Ghidiu, M. R. Lukatskaya, M. Q. Zhao, *Nature*, 2014, **516**, 78-81.

2 M. Hu, Z. Li, H. Zhang, *Chem. Commun.*, 2015, **51**, 13531-13533.

3 Y. Du, B. Yu, L. Wei, Y. Wang, X. Zhang, S. Ye, *J. Mater. Sci.*, 2019, **54**, 13283-13297.

4 Q. Peng, J. Guo, Q. Zhang, J. Xiang, B. Liu, A. Zhou, Y. Tian, *J. Am. Chem. Soc.*, 2014,**136**, 4113-4116.

5 B.M. Jun, N. Her, C.M. Park, Y. Yoon, Environ. *Sci.: Water Res. Technol.*, 2020, **6**, 173–180.

6 S. Wang, Y. Liu, Q Lu., F. Zhuang, *J. Mol. Liq.*, 2020, **297**, 11810.

7 J. Luo, K. Fu, M. Sun, *Acs. Appl. Mater. Inter.*, 2019, **11**, 38789-38797.

8 J. Guo, T. Chen, X. Zhou, *Appl. Organomet. Chem.*, 2019, **33**.

9 W. Fu, X. Wang, Z. Huang, *Sci. Total. Environ.*, 2019, **659**, 895-904.

10 P. Gu, S. Zhang, C. Zhang, *Dalton. T.,* 2019, **48**, 2100-2107.

11 F. Rouhani, A. Morsali, *Chem-Eur. J.*, 2018, **24**, 5529-5537.

12 X. Li, J. Xing, C. Zhang, *Acs. Sustain. Chem. Eng.*, 2018, **6**, 10606-10615.

13 W. Fu, Z. Huang, *Acs. Sustain. Chem. Eng.*, 2018, 6, 14785-14794.